An Ambimodal Trispericyclic Transition State and Dynamic Control of Periselectivity

Xiao-Song Xue,[†,‡,‖] Cooper S. Jamieson,[‡,‖] Marc Garcia-Borràs,[‡,‖] Xiaofei Dong,[‡,‖] Zhongyue Yang[‡,§], K. N. Houk[*,‡]

[†] *State Key Laboratory of Elemento-Organic Chemistry, College of Chemistry, Nankai University, Tianjin 300071, China*

[‡] *Department of Chemistry and Biochemistry, University of California, Los Angeles, California 90095, United States.*

Supporting Information Placeholder

ABSTRACT: We report an ambimodal trispericyclic transition state leading to [6+4]-, [4+6]-, and [8+2]-cycloadducts in the reactions of 8,8-disubstituted heptafulvenes with 6,6-dimethylfulvene. The potential energy surfaces for these reactions were explored with ωB97X-D density functional theory. Quasi-classical direct molecular dynamics simulations gave information on the ratios of products expected in these reactions.

The transition state (TS) of a reaction is a saddle point that directly connects reactants and products.[1] Over the last two decades, a number of ambimodal TSs[2] that connect one set of reactants and two different products have been discovered.[3] In such reactions, a post-transition state bifurcation (PTSB) allows the formation of two products as the reaction coordinate descends to a second transition state connecting these products without intervention of an intermediate.[3] Although transition state theory quantifies the overall rate, the product distribution is dynamically controlled.[3-4] The first ambimodal bispericyclic cycloaddition was discovered by Caramella *et al.* for the dimerization of cyclopentadiene (**Figure 1A**).[5] The authors found that a single ambimodal TS[2], followed by a PTSB, leads to identical [4+2]- and [2+4]-cycloadducts.

Since that report, reactions that involve ambimodal bispericyclic transition states have been characterized more and more frequently.[3] For example, Singleton *et al.* reported a [4+2]/[2+4] bifurcation in the cycloaddition of acrolein with methyl vinylketone (**Figure 1B**).[6] In collaboration with Singleton, we reported the SpnF-catalyzed [6+4]/[4+2] bifurcation in the biosynthesis of Spinosyn A (**Figure 1C**).[7] In collaboration with Tang, our groups characterized the Diels-Alder/hetero-Diels-Alder LepI enzyme-catalyzed bifurcation in the biosynthesis of Leporin C (**Figure 1D**).[8] All of these examples have been of ambimodal pericyclic reactions, but PTSBs also occur in other reactions,[9] including carbocation rearrangements in biosynthetic routes to terpenes that have been extensively studied by Tantillo *et al.*[10]

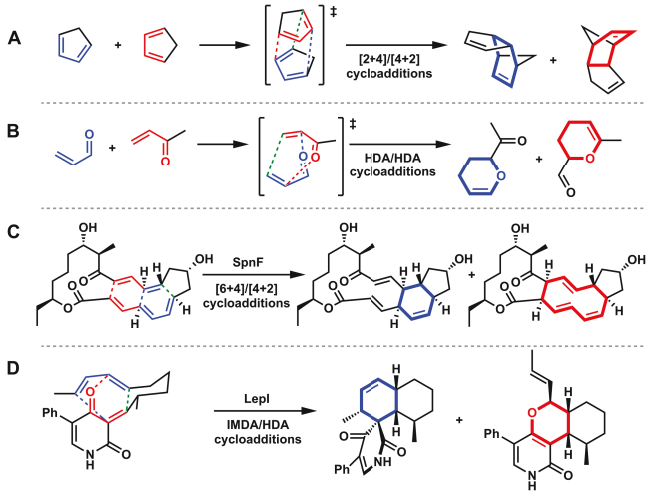

Figure 1 Representative ambimodal pericyclic reactions.

Although a transition state is a saddle point with only one direction of negative curvature,[11] there may be multiple bifurcations after the TS to give three or more products on reaction surfaces.[12]

The reactions of tropone or heptafulvenes with fulvenes can give a variety of thermally allowed cycloaddition products involving the 8π and 6π systems of the two molecules. Regioisomers and stereoisomers of [8+6], [8+2], [6+4], [4+6], [4+2], and [2+4] are possible, and we have had a long interest in understanding how periselectivity, selectivity in formation of the pericyclic-reaction products, is controlled.[13] For tropone (**1a**) and dimethylfulvene (**2a**), we have determined that products are formed from a Diels-Alder transition state and an ambiomodal TS leading to [6+4] and [4+6] adducts, to give **3**, **4**, and **5**, respectively (**Figure 2A**).[13] These transition states are favored by the electrophilic nature of C2 of tropone and nucleophilic tendency of C2 of the fulvene (**Figure 2B**).

The cycloaddition reactions of 8,8-dicyanoheptafulvene (**1b**) and 8-cyano-8-(methoxycarbonyl)heptafulvene (**1c**) with 6,6-dimethylfulvene (**2**) were studied experimentally by Liu and Ding, who found that [6+4]- and [8+2]-cycloadducts are formed (**Figure 2C**).[14] We have now explored these reactions with density functional theory (DFT) and quasi-classical direct molecular dynamics (MD) simulations and found that these primary adducts are formed from a single trispericyclic transitions state.[15]

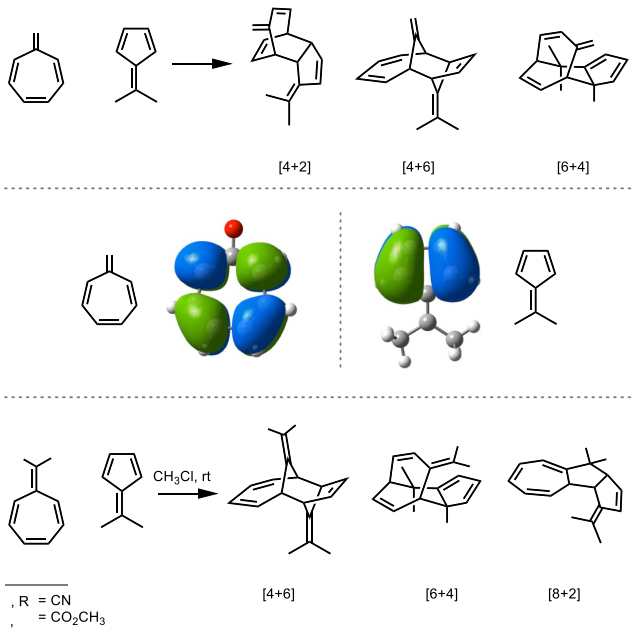

Figure 2 A. Favored cycloadditions of tropone (**1a**) and dimethylfulvene (**2**) forming [4+2], [4+6], and [6+4] adducts **B.** HOMO and LUMO of **2** and **1a**, respectively. **C.** Predicted reaction products of heptafulvenes **1b** and **1c** with 6,6-dimethylfulvene **2**.

The transition state (**TS1**) for the reaction of **1b** with **2** is shown in **Figure 3A**. **TS1** is highly asynchronous and features four partially formed σ-bonds, C1–C2, C3–C4, C5–C6, and C7–C8, with forming bond distances of 1.99, 2.77, 3.00, and 3.18 Å, respectively. Previously discovered ambimodal TS of **1a** and **2** have three partially formed σ-bonds with distances of ~ 2, 3, and 3 Å.[13d] We thus hypothesized that **TS1** is an ambimodal trispericyclic transition structure that could lead to [4+6]-, [6+4]-, and [8+2]-cycloadducts.

Quasi-classical direct dynamics simulations were initiated from **TS1**; reactants **1b** and **2** give products **6b**, **7b**, and **8b** (**Figure 3A, C, D**). Out of 142 trajectories, 123 (87%) afford the [4+6]-cycloadduct (**6b**), 4 (3%) afford the [6+4]-cycloadduct (**7b**), and 5 (3%) afford [8+2]-cycloadduct (**8b**). **Figure 3C** shows one example of each of these thre reaction trajectories. The remaining 10 (7%) trajectories recross, that is, traverse the transition zone, form the first bond (r ≤ 1.7 Å), and then returning to the other side of the TS toward reactants (or products). Analysis of trajectory path indicates that all 9 trajectories leading to **7b** and **8b** travel sequentially from **TS1** to the Cope **TS2** or **TS3**, respectively (**Figure 3C**, **D**), then continue to products. This is a general feature of ambimodal TSs.[3] The Cope TSs **TS2** and **TS3** (**Figure 6b**) interconvert the thermodynamically less stable **6b** to the more stable **7b** and **8b**, respectively. Indeed, the Cope rearrangement transition state energies are similar to the cycloaddition step. At the ωB97X-D/6-31G(d) level of theory **TS2** and **TS3** are lower than **TS1** in electronic energy by 2.7 and 1.7 kcal·mol^{-1}, respectively, although after introduction of vibrational and entropic corrections they become slightly higher in the free energy surface (**Figure 3A**, **B**).

To further characterize dynamics on this surface, 52 and 51 quasiclassical trajectories were initiated from the product interconversion Cope TSs **TS2** and **TS3**, respectively (**Figure 3**). **TS2** and **TS3** were found to be ambimodal, and both lead to the formation of **7b** and **8b** from **6b** (**Figure 3E, F**). Trajectories initiated from **TS2** or **TS3**, in one direction, pass through **TS1**, stretching C1–C2 bond from ~1.6 Å to nearly 2 Å. These trajectories can lead to separated reactants (**Figure 3E**, **F**). This is an unusual case, where **TS2** and **TS3**, each of which are typical Cope transition states by geometrical criteria, nevertheless are dynamically connected to one product and one ambimodal TS that leads also to reactants and kinetically favored product **6b**. Interestingly, the kinetically favored product is not observed experimentally, as it is thermodynamically least favored. A single trajectory from each Cope TS undergoes a formal [5,5]-sigmatropic shift and travels from **8b** to **TS3** to **TS1** to **TS2** to **7b**. Such a path traverses three transition states without intervening minima. In summary, these simulations predict that [4+6]-, [6+4]-, and [8+2]-cycloadducts are initially formed in a 25:1:1 ratio. The kinetic product occurs by formation of the secondary bond that is shortest in the ambimodal transition sate.[13d,16]

We have defined reactions to be dynamically concerted when the time-gap between bond formation (defined as ≤1.7 Å) is <60 fs and dynamically stepwise when ≥60 fs.[17] Dynamically stepwise trajectories may be energetically concerted on the potential energy surface, but proceed through an entropic intermediate[18]. The entropic intermediate is not a minimum on the PES, but has a variety of geometries with essentially the same energies that are explored before the second bond fully forms; the favorable entropy causes such a species to be a free energy minimum or intermediate. Ambimodal pericyclic reactions often involve entropic intermediates.[7a,13d] The dynamics of reaction of **1b** and **2** exhibits a bond-formation time-gap comparable to bispericyclic reactions with average time-gaps of 90, 74, and 141 fs for formation of [4+6]-, [6+4]-, and [8+2]-cycloadducts, respectively. The stationary points and entropic intermediate of trajectories for formation of kinetic product **6b** are shown in **Figure 4**.

The results for the reaction between 8-cyano-8-(methoxycarbonyl)heptafulvene (**1c**) and 6,6-dimethylfulvene (**2**) exhibit similar behaviours and are reported in the SI.

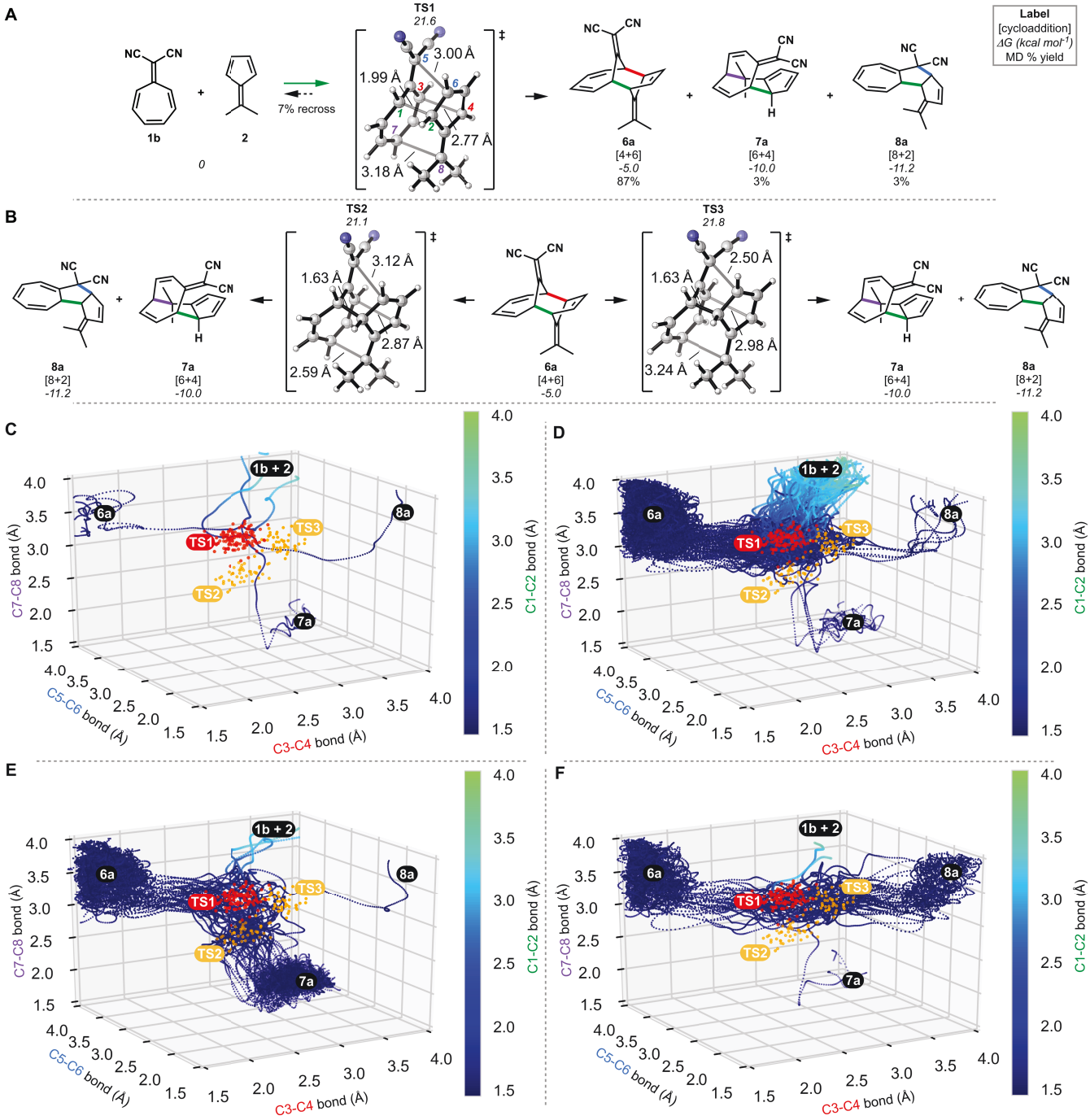

Figure 3 A. Dynamic reaction scheme of **1b** and **2** forming **6b**, **7b**, and **8b** from ambimodal trispericyclic transition structure **TS1**. **B.** Conversion of **6b** to observed products by ambimodal **TS2** and **TS3**. **C–F.** Four-dimensional plots of trajectory geometries where the common bond among products is mapped by the colorbar: separated is green (~4 Å) and formed is blue (~1.5 Å). TS ensemble geometries are overlayed in contrasting colors for clarity. **C.** Randomly selected trajectories propagated from **TS1** leading to each product. **D.** Plot of all 142 trajectories propagated from **TS1**. **E.** Plot of 52 trajectory geometries propagated from **TS2**. **F.** Plot of 51 trajectory geometries propagated from **TS3**. All calculations at the ωB97X-D/6-31G(d) level of theory.

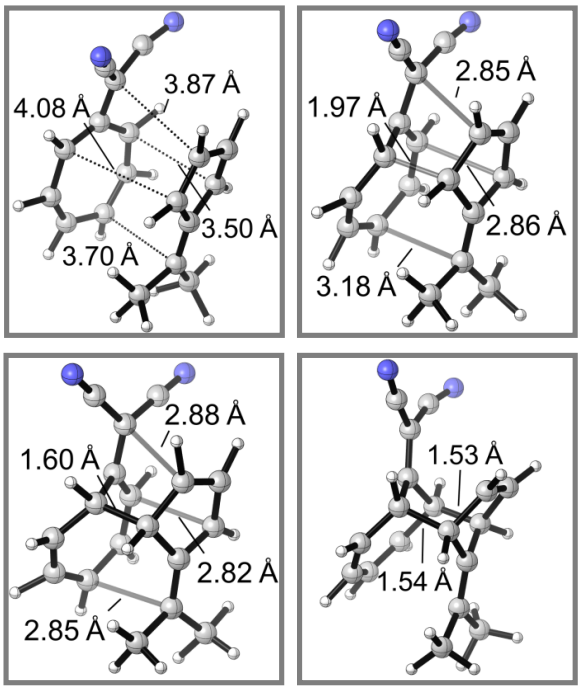

Figure 4. Snapshots of a trajectory leading from separated reactants to **TS1** to entropic intermediate to product **6b**. Refer to supporting information to see movies of trajectories.

In summary, we have characterized the [4+6]-, [6+4]-, and [8+2]-cycloaddition reactions of electron-deficient substituted heptafulvenes and 6,6-dimethylfulvene as the first identified ambimodal trispericyclic reaction. The kinetic periselectivity of the reaction is determined first by the primary bonding interactions leading most fully formed bond in the ambimodal transition state. The strongest of the three secondary orbital interactions leads through an entropic intermediate to the kinetic product while the observed products are the result of thermodynamic control. For these reactions at least, the origin of periselectivty has been understood.

ASSOCIATED CONTENT

The Supporting Information is available free of charge on the ACS Publications website.rief description (Computational Methodologies, Figure S1-S4, and optimized geometries of all species.)

AUTHOR INFORMATION

Corresponding Author

*houk@chem.ucla.edu

Present Addresses

§ Department of Chemical Engineering, Massachusetts Institute of Technology, Cambridge, Massachusetts 02139

Author Contributions

‖ These authors contributed equally.

ACKNOWLEDGMENT

We are grateful to the National Science Foundation (NSF CHE-1806581 to K. N. H) and the Natural Science Foundation of China (Grant 21772098 to X.X.S.). Calculations were performed on the Hoffman2 cluster at UCLA and the Extreme Science and Engineering Discovery Environment (XSEDE), which is supported by the National Science Foundation (OCI-1053575). X.-S. X. appreciates the hospitality provided by Professor K. N. Houk (UCLA) and wants to thank Nankai-UCLA Excellent Young Researcher program for financial support. M. G.-B. thanks the Ramón Areces Foundation for a postdoctoral fellowship.

REFERENCES

(1) Eyring, H. *J. Chem. Phys* **1935**, *3*, 107.
(2) Pham, H. V.; Houk, K. N. *J. Org. Chem.* **2014**, *79*, 8968.
(3) (a)Ess, D. H.; Wheeler, S. E.; Iafe, R. G.; Xu, L.; Celebi-Olcum, N.; Houk, K. N. *Angew. Chem. Int. Ed.* **2008**, *47*, 7592; (b)Rehbein, J.; Carpenter, B. K. *Phy. Chem. Chem. Phy.* **2011**, *13*, 20906; (c)Hare, S. R.; Tantillo, D. J. *Pure Appl. Chem.* **2017**, *89*, 679.
(4) (a)Pratihar, S.; Ma, X.; Homayoon, Z.; Barnes, G. L.; Hase, W. L. *J. Am. Chem. Soc.* **2017**, *139*, 3570; (b)Yang, Z.; Houk, K. N. *Chem. Eur. J.* **2018**, *24*, 3916.
(5) Caramella, P.; Quadrelli, P.; Toma, L. *J. Am. Chem. Soc.* **2002**, *124*, 1130.
(6) Wang, Z.; Hirschi, J. S.; Singleton, D. A. *Angew. Chem. Int. Ed.* **2009**, *48*, 9156.
(7) (a)Patel, A.; Chen, Z.; Yang, Z.; Gutiérrez, O.; Liu, H.-w.; Houk, K. N.; Singleton, D. A. *J. Am. Chem. Soc.* **2016**, *138*, 3631; (b)Yang, Z.; Yang, S.; Yu, P.; Li, Y.; Doubleday, C.; Park, J.; Patel, A.; Jeon, B. S.; Russell, W. K.; Liu, H. W.; Russell, D. H.; Houk, K. N. *Proc. Natl. Acad. Sci. U.S.A.* **2018**, *115*, E848.
(8) Ohashi, M.; Liu, F.; Hai, Y.; Chen, M.; Tang, M.-c.; Yang, Z.; Sato, M.; Watanabe, K.; Houk, K. N.; Tang, Y. *Nature* **2017**, *549*, 502.
(9) (a)Zhang, L.; Wang, Y.; Yao, Z.-J.; Wang, S.; Yu, Z.-X. *J. Am. Chem. Soc.* **2015**, *137*, 13290; (b)Hare, S. R.; Pemberton, R. P.; Tantillo, D. J. *J. Am. Chem. Soc.* **2017**, *139*, 7485; (c)Hare, S. R.; Tantillo, D. J. *Chem. Sci.* **2017**, *8*, 1442; (d)Villar López, R.; Faza, O. N.; Silva López, C. *J. Org. Chem.* **2017**, *82*, 4758; (e)Popov, S.; Shao, B.; Bagdasarian, A. L.; Benton, T. R.; Zou, L.; Yang, Z.; Houk, K. N.; Nelson, H. M. *Science* **2018**, *361*, 381; (f)Blümel, M.; Nagasawa, S.; Blackford, K.; Hare, S. R.; Tantillo, D. J.; Sarpong, R. *J. Am. Chem. Soc.* **2018**, *140*, 9291; (g)Burns, J. M. *Org Biomol Chem* **2018**, *16*, 1828; (h)Hare, S. R.; Li, A.; Tantillo, D. J. *Chem. Sci.* **2018**, DOI: 10.1039/c8sc02653j.
(10) (a)Hong, Y. J.; Tantillo, D. J. *Nat. Chem.* **2014**, *6*, 104; (b)McCulley, C. H.; Tantillo, D. J. *J. Phys. Chem. A* **2018**, *122*, 8058; (c)Hong, Y. J.; Tantillo, D. J. *J. Org. Chem.* **2018**, *83*, 3780.
(11) Stanton, R. E.; McIver, J. W. *J. Am. Chem. Soc.* **1975**, *97*, 3632.
(12) For examples: (a)Li, Y.; Houk, K. N. *J. Am. Chem. Soc.* **1996**, *118*, 880; (b)Mauksch, M.; Schleyer, P. v. R. *Inorg. Chem.* **2001**, *40*, 1756; (c)Noey, E. L.; Wang, X.; Houk, K. N. *J. Org. Chem.* **2011**, *76*, 3477; (d)Castaño, O.; Palmeiro, R.; Frutos, L. M.; Luisandrés, J. *J. Comput. Chem.* **2002**, *23*, 732; (e)Harabuchi, Y.; Nakayama, A.; Taketsugu, T. *Comput. Theor. Chem.* **2012**, *1000*, 70; (f)Harabuchi, Y.; Ono, Y.; Maeda, S.; Taketsugu, T.; Keipert, K.; Gordon, M. S. *J. Comput. Chem.* **2016**, *37*, 487.
(13) (a)Houk, K. N. Ph.D. Thesis, Harvard University, Cambridge, MA, 1964; (b)Houk, K. N.; Luskus, L. J.; Bhacca, N. S. *J. Am. Chem. Soc.* **1970**, *92*, 6392; (c)Bhacca, N. S.; Luskus, L. J.; Houk, K. N. *J. Chem. Soc. D* **1971**, 109; (d)Yu, P.; Chen, T. Q.; Yang, Z.; He, C. Q.; Patel, A.; Lam, Y.-h.; Liu, C.-Y.; Houk, K. N. *J. Am. Chem. Soc.* **2017**, *139*, 8251.
(14) (a)Liu, C. Y.; Ding, S. T. *J. Org. Chem.* **1992**, *57*, 4539; (b)Liu, C. Y.; Ding, S. T.; Chen, S. Y.; You, C. Y.; Shie, H. Y. *J. Org. Chem.* **1993**, *58*, 1628.
(15) All DFT calculations were performed using Gaussian 09. Geometry optimizations, frequency calculations and molecular dynamics were performed at the ωB97X-D/6-31G(d) level of theory. Transition structures have also been verified by intrinsic reaction coordinate (IRC) calculations. Quasiclassical trajectories were initiated from normal-mode Boltzmann-sampled TS ensembles generated using Singleton's program ProgDyn. Please refer to Supporting Information for complete computational details.
(16) Yang, Z.; Dong, X.; Yu, Y.; Yu, P.; Li, Y.; Jamieson, C.; Houk, K. N. *J. Am. Chem. Soc.* **2018**, *140*, 3061.
(17) Black, K.; Liu, P.; Xu, L.; Doubleday, C.; Houk, K. N. *Proc. Natl. Acad. Sci. U. S. A.* **2012**, *109*, 12860.

(18) Gonzalez-James, O. M.; Kwan, E. E.; Singleton, D. A. *J. Am. Chem. Soc.* **2012**, *134*, 1914.

TOC